Fuel 382 (2025) 133680

Contents lists available at ScienceDirect

Fuel

journal homepage: www.elsevier.com/locate/fuel

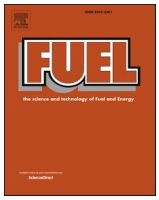

Full Length Article

Synthesis of sustainable aviation fuels via (co–)oligomerization of light olefins

Constantin Fuchs, Ulrich Arnold *, Jörg Sauer

Institute of Catalysis Research and Technology (IKFT), Karlsruhe Institute of Technology (KIT), Hermann-von-Helmholtz-Platz 1, 76344 Eggenstein-Leopoldshafen, Germany

ARTICLE INFO

Keywords:
Sustainable aviation fuels
Methanol
Olefins
Oligomerization
Heterogeneous catalysis
Renewable fuels

ABSTRACT

Within this study, the (co–)oligomerization of methanol-based olefins in the C_{2-4} range was investigated. The main objective was to increase the yield of oligomers with carbon chain lengths in the range of kerosene (C_{9-16}). Commercially available mesoporous amorphous mixed silicon-aluminum oxides, optionally modified with nickel species, were applied as catalysts. Initially, single olefin feeds were employed, i.e. homo-oligomerization reactions of pure propylene and pure 1-butylene were studied at 120 °C and 32 bar olefin partial pressure, respectively. The co-oligomerization of olefin mixtures (C_{3+4} and C_{2+3+4}), which can be obtained in Methanol-to-Olefins (MtO) processes, yields product mixtures with reduced selectivities to specific chain lengths. However, selectivities to kerosene-like olefins up to 85 % have been achieved and the main side product is gasoline. Investigations with varying reaction conditions reveal comparable effects as in the case of homo-oligomerization. The use of nickel-free catalysts resulted in the highest selectivities of kerosene-like olefins, but no ethylene was converted. The negative effects of nickel catalysts on fuel quality can be compensated by two consecutive catalyst beds, the first catalyst bed with a nickel-loaded silicon-aluminum oxide for ethylene conversion followed by a catalyst bed of neat silicon-aluminum oxide for the synthesis of highly branched, long chain oligomers. The reaction network for olefin oligomerization reactions is depicted, which can be simplified remarkably in the case of catalysts without nickel. A long-term experiment lasting for more than 200 h was conducted revealing a deactivation of the acid sites of the catalysts, but also the possibility of reactivation. Selectivity to kerosene-like olefins remained above 63 % and fuel characterization showed that the resulting kerosene fraction will be suitable for blending with conventional fuels.

1. Introduction

In aviation, electrification of propulsion is very challenging. Today, batteries are heavy and moreover, do not offer as high energy densities as liquid fuels. As a consequence, electrically driven aircrafts will not reach the transport distances and capacities of the current aircraft fleets using fossil liquid fuels. Therefore, the defossilization of the aviation sector requires renewable fuels produced from sustainable sources [1].

Sustainable aviation fuels (SAF) can be produced in several ways [2–4]. One way is to convert biomass to hydro-treated esters and fatty acids (HEFA). Another method is to produce synthetic paraffinic kerosene (SPK) [5]. This can be done by Fischer-Tropsch synthesis with downstream hydrocracking and hydrotreatment [6]. Alternatively, the alcohol-to-jet route (ATJ) can be chosen, involving alcohol dehydration to olefins, olefin oligomerization and hydrogenation [7,8]. All these fuels are free of aromatics. As aromatics lead to particle formation during combustion and particles favor cloud formation in the atmosphere, the impact on global warming of such non-CO_2 effects can be larger than the impact of CO_2 emitted during fuel combustion [9,10]. Consequently, processes for the synthesis of sustainable aviation fuels, which are free of aromatics, can contribute to reducing the environmental impact of aviation.

As the provision of biomass for large-scale plants has been difficult to

Abbreviations: ASTM D7566, Jet-fuel standard according to American Society for Testing and Materials; ATJ, Alcohol-to-Jet; BET, Brunauer-Emmett-Teller; BS, Brønsted acid site; BJH, Barrett-Joyner-Halenda; DME, Dimethyl ether; DIN EN 228, Gasoline standard according to Deutsches Institut für Normung; DtO, DME to Olefins; FT, Fischer-Tropsch; FTIR, Fourier-transform infrared spectroscopy; GC, Gas chromatography; HEFA, Hydro-treated esters and fatty acids; MtO, Methanol to Olefins; MOGD, Mobil Olefins to Gasoline and Distillate; NH_3-TPD, Ammonia temperature programmed desorption; RON, Research octane number; SAF, Sustainable aviation fuel; SPK, Synthetic paraffinic kerosene; TOS, Time on stream.

* Corresponding author.
E-mail address: ulrich.arnold@kit.edu (U. Arnold).

https://doi.org/10.1016/j.fuel.2024.133680
Received 28 August 2024; Received in revised form 25 October 2024; Accepted 7 November 2024
Available online 21 November 2024

Nomenclature

Symbols used

C_y	[-] Olefin with y carbon atoms
d_{Pore}	[nm] Pore diameter
I_{iso}	[-] Isoindex of the C_8 fraction
$N_{Brønsted\ sites}$	[µmol/m^2] Density of Brønsted acid sites
p	[bar] Pressure
r	[mol_{Olefin}/(µmol BS·s)] Reaction rate per Brønsted acid site and second
S_{BET}	[m^2/g] Specific surface
T	[°C] Temperature
V_{Pore}	[ml] Pore volume
$WHSV$	[h^{-1}] Weight hourly space velocity
$x_{z\text{-branched}}$	[-] Share of z-fold branched octenes in the C_8 fraction (z = single, double and triple)
X_{Cy}	[%] Conversion of olefin with y carbon atoms
$S_{Gasoline}$	[%] Selectivity to gasoline
$S_{Kerosene}$	[%] Selectivity to kerosene

implement so far, power-to-liquid processes like Fischer-Tropsch synthesis or alcohol-based olefin oligomerization are steadily gaining attraction due to further developments and scale-up in the provision of synthesis gas, e.g. via CO_2 from direct air capture and H_2 from water electrolysis with renewable energies. The Fischer-Tropsch synthesis achieves selectivities to jet fuel of less than 40 % [11] and requires a hydrocracking step downstream [12]. A very promising pathway is the methanol- or dimethyl ether (DME)-based ATJ process. This pathway comprises several conversion steps and allows for a targeted synthesis of jet fuel with selectivities of more than 70 % [4,13]. At first, methanol or DME made from green hydrogen and CO_2 is converted to olefins and water in a Methanol/DME-to-Olefins process (MtO/DtO). The current state of the art is the conversion in fluidized bed reactors with continuous catalyst regeneration by burning off the coke [14,15]. The main hydrocarbon products are light olefins in the range of $C_{2\text{-}4}$. Recently, the production of higher olefins in the range of $C_{5\text{-}9}$ by modified MtO/DtO processes was shown by Niethammer et al. [16].

The subsequent olefin oligomerization is the crucial step for the production of jet fuel. The oligomerization reaction can be understood as a polymerization reaction, which terminates after the coupling of a few monomers [17]. The product spectrum covers the entire carbon chain length range from gasoline to kerosene and diesel fuel. By varying the process parameters, the desired fuel fraction can be produced in a targeted manner [13,18,19]. If olefin mixtures are used as feed, the reaction is referred to as co-oligomerization. After (co–)oligomerization, the liquid oligomers need to be hydrogenated leading to a purely paraffinic hydrocarbon mixture usable as gasoline, jet fuel and diesel fuel after separation of the fractions by distillation.

The oligomerization of individual olefin species is well-known from literature. The conversion of ethylene [18–26], propylene [27–36] or 1-butylene [13,37–42] has been investigated with various catalysts under varying reaction conditions. In the past, the focus has been primarily on the homogeneously catalyzed oligomerization of ethylene using for example metal complexes as catalysts. With transition metals like nickel, the oligomerization of ethylene proceeds at comparably low temperatures of less than 150 °C via a coordination-insertion mechanism according to Cossee and Arlmann [18,19,22,43]. In this temperature range, it is the dominant reaction pathway for ethylene conversion, leading preferentially to linear and single-branched molecules [20]. However, the products exhibit poor cold flow properties and are typically applied as lubricants or intermediates for the synthesis of polyethylene [44–46]. For applications in the field of aviation fuel, the cold flow properties of the fuel are crucial [47], which can be improved by high degrees of branching in the molecules [48]. Brønsted acid sites on heterogeneous catalysts offer the possibility for a targeted synthesis of branched oligomers. At Brønsted acid sites, carbenium ions are formed leading to chain growth and isomerization reactions [49]. Metathesis reactions are also occurring. In contrast to ethylene, higher olefins with a carbon chain length of C_{3+} form carbenium ions at Brønsted acid sites and do not require any activation of the oligomerization reaction by transition metals. Ultimately, the acid site-catalyzed reaction pathway leads to higher degrees of branching and better cold flow properties of the produced kerosene. Additionally, a high branching enhances quality of the by-product gasoline, especially its knock resistance [50].

For heterogeneously catalyzed oligomerization reactions on Brønsted acid sites, different types of catalysts like aluminosilicates, zeolites, resins, supported phosphoric acid or metal–organic frameworks have been investigated so far [51–54]. Mesoporous, amorphous silica-alumina catalysts with a moderate density of Brønsted acid sites showed the best performance regarding olefin conversion, selectivity to fuel range oligomers and resistance against deactivation by coking [13,19,26,53,55,56].

In industry, processes for fuel production by olefin homo-oligomerization have already been developed. As an example of kerosene synthesis from renewable olefins, GEVO has developed an alcohol-to-jet process using isobutylene as an olefin monomer [57]. At first, isobutanol is produced through fermentation, which is then converted to isobutylene by dehydration. Subsequently, isobutylene is oligomerized to its trimer isododecene. After hydrotreatment, the isododecane can be blended with commercial kerosene [57]. In the last century, the co-oligomerization of olefin mixtures has been demonstrated by UOP in the Catpoly process [54] as well as by Mobil in the “Mobil Olefins to Gasoline and Distillate” (MOGD) process [58]. The MOGD process uses a mixture of $C_{2\text{-}4}$ olefins, representative of a product mixture from ExxonMobil’s MtO process [59]. In the case of the Catpoly process, propylene and butylene are converted to highly branched aviation gasoline [60]. Furthermore, the Polynaphtha process developed by Axens IFP converts $C_{3\text{-}5}$ olefins to oligomeric gasoline and gas oil. By recycling the oligomeric gasoline back into the oligomerization reactor, the yield of longer oligomers in the kerosene range can be increased. However, none of the mentioned co-oligomerization processes is currently operated on a large scale for fuel production due to economic reasons. Furthermore, current research and literature rarely focus on the co-oligomerization of multiple olefin species as feedstock, although the technology offers great potentials for the synthesis of low emission fuels. Nowadays, industry is gradually recognizing these potentials for example in the context of sustainable aviation again.

This is the starting point for the present study. Since the co-oligomerization of olefins has not been systematically developed for decades, this study focuses on the production of kerosene from $C_{2\text{-}4}$ olefins and mixtures thereof. The employed catalysts are not within the focus as they have been selected and described in previous studies [13,19]. The main objective is to disclose the influence of feed compositions, e.g. by comparison of homo- and co-oligomerization, and to estimate the obtainable product spectra and their properties.

More specifically, differences in the homo-oligomerization of propylene and 1-butylene to kerosene were revealed, which is a direct continuation of previously reported work [13]. Afterwards, the co-oligomerization of olefin mixtures was investigated regarding several reaction conditions, which was not addressed in the past. The synthesis of kerosene on nickel-loaded and nickel-free silica-alumina catalysts was studied revealing the possibility of a selective co-oligomerization from olefin mixtures with and without ethylene conversion. To overcome the negative effects of nickel-catalyzed ethylene oligomerization on the molecular branching of the oligomers, two consecutive catalyst beds were employed containing a nickel-loaded catalyst and a nickel-free catalyst. Variations of the apparent reaction mechanisms were used to display variations in the (co–)oligomerization reaction network, which can support simplified predictions of product distributions in the future.

Finally, in a long term co-oligomerization experiment lasting for 200 h the catalyst stability was investigated. The produced kerosene and gasoline fractions were characterized with respect to their physico-chemical properties and catalyst deactivation and regeneration were addressed.

2. Materials and methods

A commercially available mesoporous silica-alumina, SIRALOX 40 from Sasol, was used as catalyst and catalyst support. The material without nickel loading is abbreviated as 40/0Ni. The value 40 represents the percentage of silicon oxide, consequently 60 % is aluminum oxide. In addition to the blank catalyst, a catalyst loaded with 2 wt% of nickel was prepared, which is referred to as 40/2Ni in the following. In previous studies, this catalyst proved to be the most suitable one [13,19]. For the preparation of the nickel-loaded catalyst, SIRALOX 40 was first calcined at 550 °C for 8 h. Nickel was loaded using the incipient wetness impregnation method. A nickel salt solution of $Ni(NO_3)_2{\cdot}6\ H_2O$ (99.9 % from ABCR) was prepared with distilled water and added to the support. After drying at 50 °C and subsequent calcination at 550 °C, a particle size of 250 to 500 µm was adjusted by sieving.

Both catalysts were examined for their surface properties using nitrogen physisorption. Nitrogen isotherms were recorded at 77 K using a Novatouch 4LX analyzer (Quantachrome Instruments). Based on nitrogen desorption, the specific surface area (S_{BET}) was calculated using the Brunauer-Emmett-Teller (BET) method in the relative pressure range (p/p_0) from 0.002 to 0.3. The mean pore diameter (d_{Pore}) and the specific pore volume (V_{Pore}) were determined using the Barrett-Joyner-Halenda (BJH) method. Acidity of the catalysts was measured by NH_3-TPD employing an AutoChem 2950 HP from Micromeritics. Fourier Transform Infrared (FTIR) spectroscopy was performed on a Bruker Tensor 27 instrument at LIKAT Rostock. Pyridine was used as a probe molecule and by this, a distinction could be made between Lewis and Brønsted acid sites. The density of Brønsted acid sites ($N_{Brønsted\ sites}$) plays an important role in the oligomerization reaction, as the C_{3+} olefins form carbenium ions at these sites and initiate carbon chain growth.

Some properties of the bare (40/0Ni) and the nickel-loaded (40/2Ni) catalyst are summarized in Table 1. The number of weak Brønsted acid sites was determined by pyridine adsorption FTIR spectroscopy at 200 °C. It is shown that the nickel loading reduces the overall surface of the catalyst, the median pore diameter as well as the pore volume. In addition, 2 wt% nickel on the support reduces the density of Brønsted acid sites by almost 27 % through the deposition of nickel. The support materials SIRALOX 20 and 70 as well as the corresponding nickel-loaded catalysts were also investigated and their surface properties can be found in Table S1 in the Supplementary Information. For further information on nickel-catalyzed oligomerization, we refer to prior studies of Betz et al. [19] and Fuchs et al. [13].

A detailed description of the continuously operating oligomerization plant, the fixed bed reactor and the experiments is provided by Betz et al. [19] and Fuchs et al. [13]. Previous oligomerization experiments have shown that a temperature of 120 °C and a total pressure of 40 bar lead to good results in terms of conversion, selectivity and branching of the liquid oligomers [13,19]. As the catalysts are of medium acidity and the reaction temperature of 120 °C is quite low, side reactions like cyclization, aromatization or the hydrogenation of olefins to paraffins are suppressed. Consequently, the product contains only olefins. Therefore, these conditions were also applied within this study. As educts, ethylene (99.9 %, Air Liquide), propylene (99.5 %, Air Liquide) and 1-butylene (99.4 %, Air Liquide) were utilized. For each experiment, 5 g of fresh catalyst were used. To enable an isothermal operation of the reactor, the catalyst was mixed with the tenfold volume of silicon carbide. Co-oligomerization experiments were conducted with equimolar shares of propylene and 1-butylene as well as with a MTO product surrogate. As the compositions of the olefin mixtures from the MTO process depend on catalysts and process conditions, the surrogate mixture applied in this study contains 40 vol% ethylene, 40 vol% propylene and 20 vol% 1-butylene [61–64]. Conversions of the individual olefins were determined by online GC analysis, which provides volume flows of the olefins. For ethylene and propylene this was achieved simply by calculating the difference between input and output. Butylene conversions were calculated according to the same procedure. However, for butylene no proper determination of conversions is possible in the co-oligomerization experiments, as ethylene is dimerized to butylenes on nickel sites (see Section 3.2.2.). Thus, the true conversion of the fed butylene is veiled. An olefin partial pressure of 32 bar was chosen, and the total pressure was maintained at 40 bar, as argon (99.999 %, Air Liquide) was applied as an inert gas to serve as a reference for online gas analysis. The argon content in the feed amounted to 20 vol%. The quantification of gaseous products was performed using an online gas chromatograph HP 5890 equipped with an Rt-Alumina BOND/Na_2SO_4 column. The liquid hydrocarbons were determined offline using an Agilent GC6890 with a DB-1 column. The determination of the chain length distributions, enabling the assignment to gasoline ($C_{5\text{-}10}$) and kerosene ($C_{9\text{-}16}$), was achieved through simulated distillation. The degree of branching was also determined by GC analysis. For this purpose, a subsequent hydrogenation, employing palladium catalysts at 80 °C and 30 bar hydrogen pressure, was conducted according to Heveling et al. [65]. This hydrogenation leads to the elimination of stereoisomers and is essential for determining the branching within the liquid products. As an indicator for branching and gasoline quality, the isoindex for the C_8 fraction was determined in the case of 1-butylene oligomerization and the co-oligomerizations of olefin mixtures. The isoindex I_{iso} indicates the average number of branchings in octane molecules and is calculated with the mass-related shares x of the branched octanes according to the subsequent formula.

$$I_{iso} = x_{triple-branched}{\cdot}3 + x_{double-branched}{\cdot}2 + x_{single-branched}$$

Linear octenes are not considered. For gasoline applications, the isoindex should be close to 3 representing triple-branched molecules like isooctane with research octane numbers of around 100. It has to be considered that the knocking resistance drops significantly with a lower degree of branching [50]. However, Dagle et al. showed that also double-branched octenes, viz. dimethylhexenes, can be blended up to 20 wt% to conventional gasoline without a loss of knocking resistance [66]. Consequently, the isoindex of the octenes should be in the range of 2 to 3 to provide a sufficiently high-quality blending component. Since the C_8 fraction in propylene oligomerization does not represent an integer multiple of the propylene monomer, C_8 is exclusively formed through rearrangement reactions such as metathesis. Therefore, it is present only in very small amounts and thus, the isoindex was not calculated for the products from propylene oligomerization experiments.

A long-term experiment allowed for the analysis of fuel properties, which was performed for a kerosene fraction and a gasoline fraction at ASG Analytik Service AG according to certified testing methods. By distillation of the total product mixture, it is not possible to make a clear distinction regarding chain lengths, as the boiling ranges are blurred due to isomers and other effects like boiling delay. This means that hydrocarbons outside the chain lengths defined above may also be present in small proportions in the fuels, e.g. a C_{12} oligomer in the gasoline or C_7 and conceivable diesel components in the kerosene fraction.

Table 1
Surface properties of metal-free 40/0Ni and nickel-loaded 40/2Ni.

Catalyst	S_{BET} [m^2/g]	d_{Pore} [nm]	V_{Pore} [ml/g]	$N_{Brønsted\ sites,\ 200\ °C}$ [µmol/g]
40/0Ni	455	9.2	1.57	46.8
40/2Ni	373	7.1	1.14	35.4

3. Results and discussion

3.1. Homo-oligomerization of propylene and 1-butylene

In the first step, feeds composed of one olefin and their homo-oligomerization were investigated. The focus was on the oligomerization of propylene and 1-butylene, respectively since ethylene oligomerization has been widely investigated in the past [19]. Furthermore, reaction parameters such as temperature and pressure have already been considered [13] and here, previous work is complemented by investigations on space velocity and a direct comparison of catalysts with and without nickel.

3.1.1. Effect of space velocity on propylene and 1-butylene homo-oligomerization catalyzed by 40/0Ni

The residence time can play an important role regarding the degree of oligomerization and the product distribution. Therefore, the effects of varying weight hourly space velocity (WHSV) on olefin conversion and selectivity to kerosene as well as gasoline were investigated with the blank catalyst SIRALOX 40 (40/0Ni). The olefin conversions for a WHSV of 2, 4 and 8 h^{-1} are shown in Table 2. The longest residence time represented by a WHSV of 2 h^{-1} reveals highest conversions for propylene and 1-butylene. With increasing WHSV, conversions decrease and the drop in propylene conversion is significantly higher than in 1-butylene conversion.

The correlation of olefin conversion with the number of Brønsted acid sites of the catalyst allows for a better comparison regarding the reactivity of propylene and 1-butylene. The corresponding reaction rates *r* in terms of molar olefin conversion per Brønsted acid sites of the catalyst and time were calculated for the three investigated WHSVs (Fig. 1). At a WHSV of 2 h^{-1}, an almost complete conversion of propylene and 1-butylene is achieved (Table 2) and molar propylene consumption is higher than 1-butylene consumption (Fig. 1). Doubling the WHSV to 4 h^{-1} results in an approximately threefold increase of molar 1-butylene consumption while a maximum is reached in the case of propylene. A further increase to a WHSV of 8 h^{-1} shows another strong increase of 1-butylene consumption. In contrast, molar propylene consumption is slightly decreasing.

The reason for the observed differences is the formation of different carbenium ions, which are crucial for the oligomerization reaction. The higher reactivity of 1-butylene compared to propylene can be attributed to the higher stability of secondary carbenium ions. These are stabilized by inductive effects (+I effect) of the substituents and, for instance, ethyl groups provide stronger + I effects than methyl groups [67]. At a reaction temperature of 120 °C, 1-butylene can undergo isomerization to 2-butylene due to thermodynamic equilibrium. In this case, the secondary carbenium ion of 2-butylene is substituted with an ethyl and a methyl group, while in the case of propylene, the substituents are two methyl groups. Another indication of the increased stability of butylene carbenium ions is the enthalpy released during hydrogenation to the corresponding paraffins [68]. The less enthalpy is released, the more stable is the olefin and its associated carbenium ion [69]. For propylene, the enthalpy of hydrogenation is −123.4 kJ/mol [70], while for *trans*-2-butylene, it is −114.6 kJ/mol and −118.5 kJ/mol for *cis*-2-butylene [71].

The selectivities to gasoline ($C_{5\text{-}10}$) and kerosene ($C_{9\text{-}16}$) of the C_3 and C_4 oligomerizations are differentiated by chain length and listed in Table 3. Comparing the different feedstocks, propylene offers higher selectivities to kerosene fractions of more than 90 %. 1-Butylene oligomerization reveals selectivities of around 70 % for lower WHSV. This difference occurs from the dimerization of 1-butylene and the high C_8 content, which is not assigned to the kerosene fraction. While 1-butylene oligomerization leads to similar kerosene selectivities for a WHSV of 2 and 4 h^{-1} at 8 h^{-1} kerosene selectivity decreases to 52 % and gasoline selectivity increases to about 53 %. This behavior is also known from previous work in the field of ethylene oligomerization [18,65,72,73]. Regarding propylene oligomerization, selectivities to C_{9+} olefins of above 90 % were reached in every experiment. Consequently, its selectivity to kerosene is almost independent of the residence time, which is explained in the following.

The product distributions in terms of chain length were determined for propylene and 1-butylene oligomerization at a WHSV of 2, 4 and 8 h^{-1} (Fig. 2). Integer multiples of the monomers are primarily formed, while deviations in chain length can be attributed to metathesis reactions on the acidic support [20]. Even though the selectivity to kerosene is almost constant in the case of propylene oligomerization (Table 3), carbon chain lengths within the $C_{9\text{-}13+}$ fraction shift to shorter chain lengths with increasing WHSV, mainly to C_9. Since the proportions of oligomers $C_{<9}$ do not increase significantly and due to the defined range for kerosene, the selectivity for kerosene does not decrease with increasing WHSV. This shift is also observed in 1-butylene oligomerization and explains the decrease of selectivity to kerosene by increased formation of octenes at a WHSV of 8 h^{-1}. It is evident that longer

Table 2
Conversions of propylene and 1-butylene as a function of WHSV (Reaction conditions: T = 120 °C, $p_{Olefins}$ = 32 bar, p_{total} = 40 bar, TOS = 4h).

WHSV [h^{-1}]	X_{C3} [%]	X_{C4} [%]
2	97.8	96.6
4	69.7	94.7
8	32.5	85.8

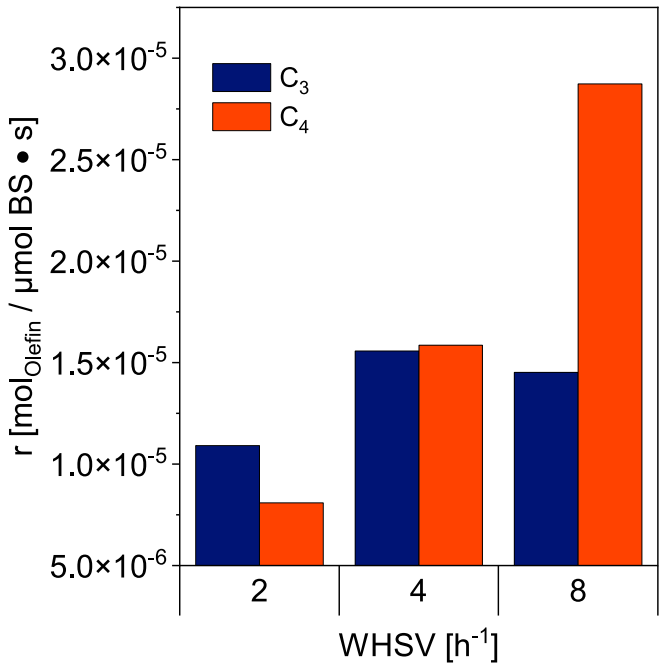

Fig. 1. Reaction rate *r* of molar propylene and 1-butylene conversion per Brønsted acid sites of the catalyst and second (Reaction conditions: T = 120 °C, $p_{Olefins}$ = 32 bar, p_{total} = 40 bar).

Table 3
Selectivity to gasoline ($C_{5\text{-}10}$) and kerosene ($C_{9\text{-}16}$) in propylene and 1-butylene oligomerization for a WHSV of 2, 4 and 8 h^{-1} (Reaction conditions: T = 120 °C, $p_{Olefins}$ = 32 bar, p_{total} = 40 bar).

WHSV [h^{-1}]	C_3 oligomerization		C_4 oligomerization	
	$S_{Gasoline}$ [%]	$S_{Kerosene}$ [%]	$S_{Gasoline}$ [%]	$S_{Kerosene}$ [%]
2	27.5	92.8	35.0	71.1
4	40.2	93.5	36.4	70.9
8	48.8	92.5	53.2	52.4

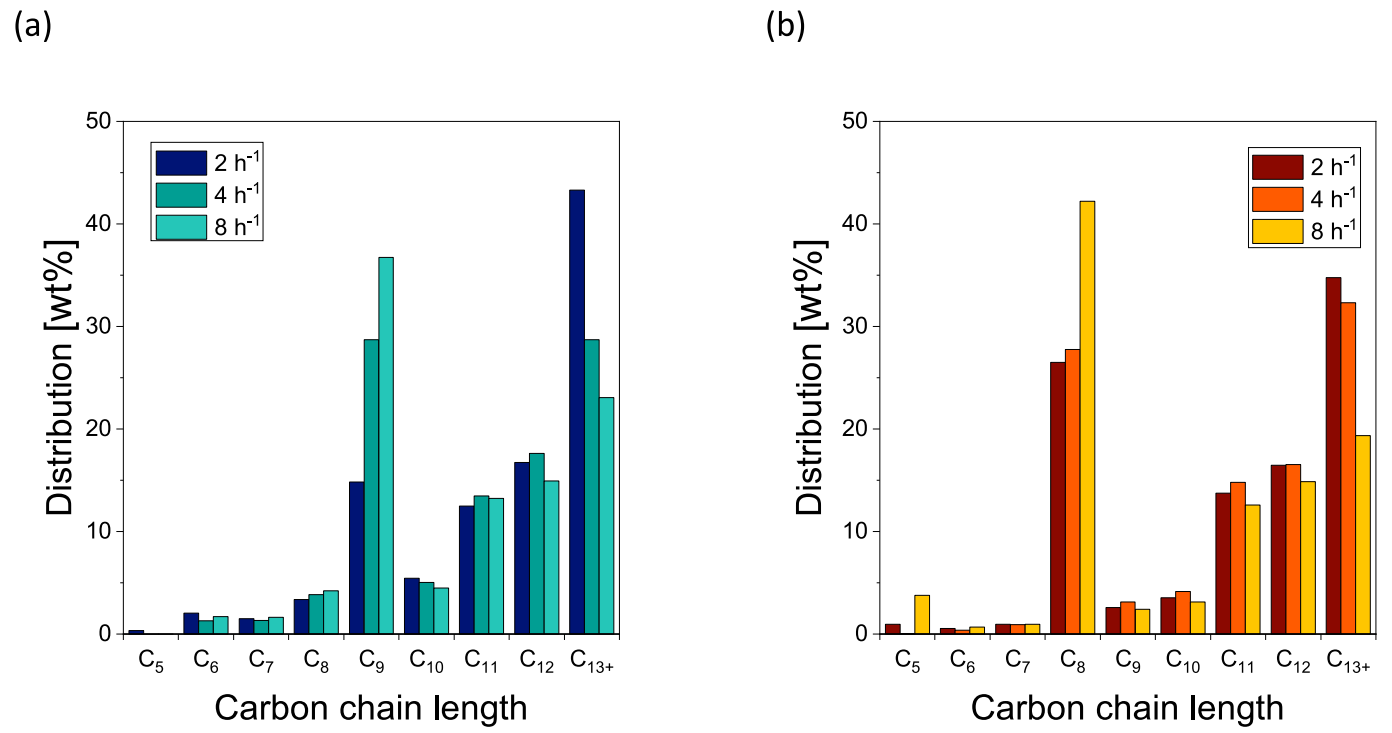

Fig. 2. Product distributions as a function of WHSV for (a) propylene and (b) 1-butylene oligomerization (Reaction conditions: T = 120 °C, $p_{Olefins}$ = 32 bar, p_{total} = 40 bar).

residence times (lower WHSV) are advantageous for shifting the product spectrum towards higher oligomers in the kerosene range [18,74]. However, it should be noted that higher oligomers in the diesel fuel range and deposits on the catalysts can also be formed. This can promote a faster deactivation of the catalyst due to the blockage of catalytically active sites [39]. By increasing the temperature under an inert atmosphere to remove soft coke or by burning off the hard coke deposits with oxygen, the catalyst can be regenerated [13]. Consequently, after longer residence times, shorter regeneration intervals are necessary for restoring the original catalyst activity.

In summary, at the highest WHSV of 8 h^{-1}, the conversion of propylene per Brønsted acid site decreases significantly and furthermore, the selectivity to kerosene in 1-butylene oligomerization is reduced. This behavior is also observed for the SIRALOX 20 catalysts, as shown in the Supplementary Information (Figs S1 and S2, Tables S2 to S4). Consequently, a WHSV of 4 h^{-1} is considered as particularly suitable and this WHSV was chosen for the subsequent studies.

3.1.2. *Effect of nickel loading on propylene and 1-butylene homo-oligomerization*

Nickel loading on the catalysts provides additional active sites and as already mentioned above, also influences properties of the support material like the density of acid sites. Therefore, catalytic performance changes and enables tuning of the product distributions and thus, fuel properties. In the first step, conversions of propylene and 1-butylene were determined for both catalysts, 40/0Ni without and 40/2Ni with nickel loading (Table 4). Furthermore, product spectra for propylene and 1-butylene oligomerization were determined for both catalysts (Fig. 3).

Table 4
Conversions of propylene and 1-butylene for 40/0Ni and 40/2Ni (Reaction conditions: T = 120 °C, WHSV = 4h^{-1}, $p_{Olefins}$ = 32 bar, p_{total} = 40 bar).

Catalyst	$X_{Propylene}$ [%]	$X_{1\text{-}Butylene}$ [%]
40/0Ni	69.7	94.7
40/2Ni	85.9	87.2

Regarding conversion, nickel impregnation increases the conversion of propylene while the conversion of 1-butylene decreases. In this respect, it can be concluded that propylene, similar to ethylene, reacts at nickel sites through the insertion-coordination mechanism [75] in addition to reactions at the Brønsted acid sites [76]. On the other hand, 1-butylene preferably reacts at Brønsted acid sites. Since these can be partially occupied by nickel species [65], their density decreases resulting in a decrease of 1-butylene conversion. The decrease of Brønsted acid sites is already shown in Table 1. Additionally, Tables S3 and S4 confirm this effect for the 20/0Ni and 20/2Ni catalysts.

In the case of propylene oligomerization (Fig. 3(a)), there is only a minor effect of nickel loading on the product distribution, which can be explained by the acid and nickel site catalyzed reactions of propylene. In contrast, the influence of nickel loading is clearly reflected in 1-butylene oligomerization. With nickel impregnation, the product distribution shifts significantly towards shorter chain lengths, primarily towards the dimer octene (Fig. 3(b)). Additionally, the fraction of C_{13+} is reduced to less than half.

The corresponding selectivities to gasoline and kerosene and, in the case of C_4 oligomerization, the isoindex are also given (Table 5). Compared to 1-butylene oligomerization, propylene oligomerization yields higher selectivities to oligomers with carbon chain lengths of C_{9+} and overall the highest selectivities to kerosene for both catalysts. Since 1-butylene oligomerization results in dimerization to C_8, the selectivity to kerosene is lower in this case due to the confinement of kerosene to the range of $C_{9\text{-}16}$. Regarding the selectivities to gasoline and kerosene, the influence of nickel is minimal in the case of propylene (Table 5). On the other hand, the proportion of kerosene in 1-butylene oligomerization is significantly reduced due to the shift of the product distribution towards C_8. This effect is also visible for the catalysts 20/0Ni and 20/2Ni (Fig. S3), as well as 70/0Ni and 70/2Ni (Fig. S4). Next to the carbon chain length distribution, nickel loading has also an impact on the degree of molecular branching [24]. Without nickel, the isoindex is 1.99, indicating that, on average, each octene molecule is approximately double-branched. However, with nickel, the average branching degree is

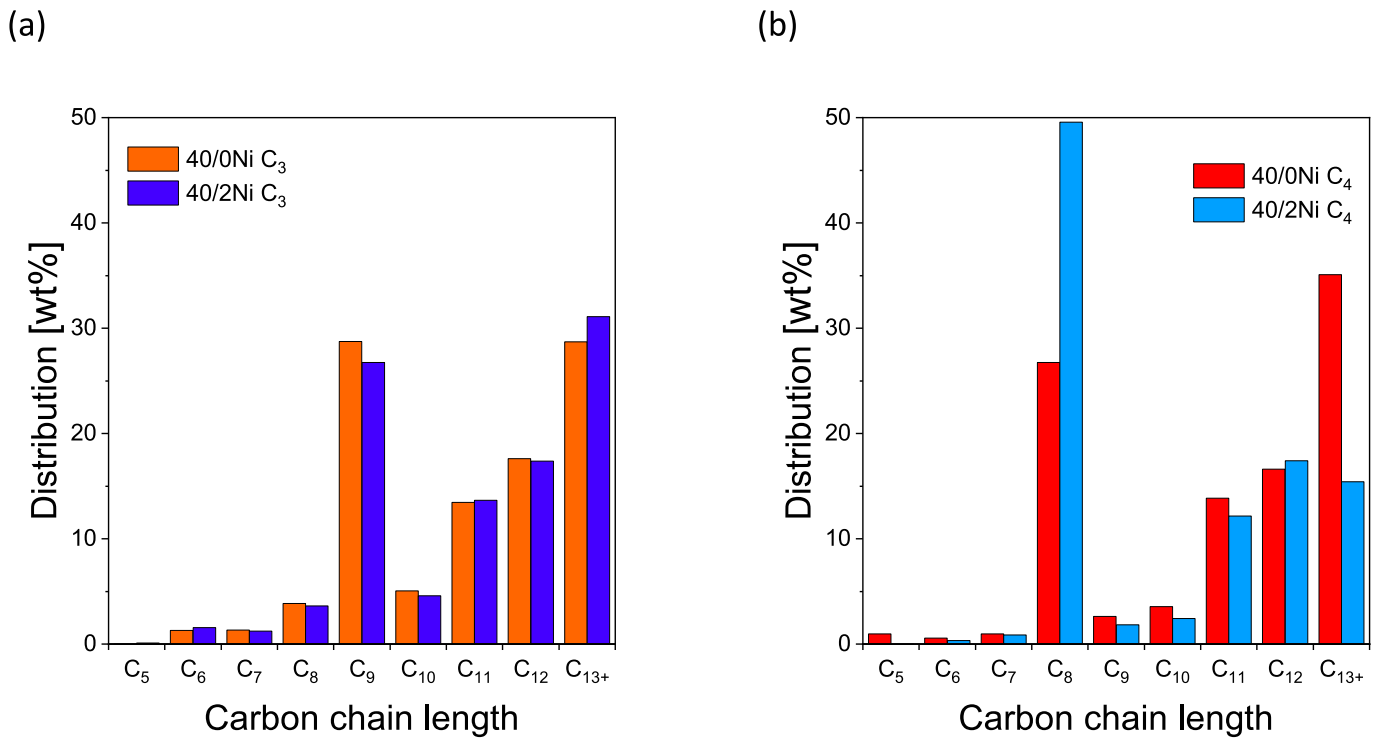

Fig. 3. Product distributions of 40/0Ni and 40/2Ni for (a) propylene and (b) 1-butylene oligomerization (Reaction conditions: T = 120 °C, WHSV = $4h^{-1}$, $p_{Olefins}$ = 32 bar, p_{total} = 40 bar).

Table 5
Selectivity in propylene and 1-butylene oligomerization over 40/0Ni and 40/2Ni (Reaction conditions: T = 120 °C, WHSV = $4h^{-1}$, $p_{Olefins}$ = 32 bar, p_{total} = 40 bar).

Catalyst	C_3 oligomerization		C_4 oligomerization		
	$S_{Gasoline}$ [%]	$S_{Kerosene}$ [%]	$S_{Gasoline}$ [%]	$S_{Kerosene}$ [%]	I_{iso} C_8
40/0Ni	40.2	93.5	35.4	71.8	1.99
40/2Ni	37.9	93.5	55.0	49.2	1.93

reduced to 1.93, resulting from higher proportions of linear and single-branched octenes. This is due to the nature of nickel to form rather linear molecules [22,43]. This loss in the average branching degree can already significantly reduce the octane rating of the produced gasoline as linear and single-branched octenes exhibit low knocking resistances [50].

3.2. Co-oligomerization of olefin mixtures

In addition to feeds composed of one olefin and their homo-oligomerization, co-oligomerization of mixed olefin feeds, similar to product mixtures from MtO processes, was also investigated. Since compositions can be varied over a wide range, product spectra and properties can be influenced to a large extent. Correlations between feeds, catalysts, reaction conditions and the resulting products are described in the following.

3.2.1. Co-oligomerization of $C_3 + C_4$ and $C_2 + C_3 + C_4$ olefin mixtures

To investigate the influence of different olefin feeds on kerosene yield, two different olefin mixtures were examined. Initially, a binary mixture of propylene and 1-butylene in an equimolar ratio was oligomerized, followed by the oligomerization of a ternary mixture of ethylene, propylene and 1-butylene surrogating a typical product mixture of a MtO process. The olefin feed composition in the latter case is 40 mol% ethylene, 40 mol% propylene and 20 mol% 1-butylene. Analogous to Chapter 3.1., conversions, selectivities and isoindices were determined and results are summarized in Tables 6 and 7 and Fig. 5. In the Supplementary Information, Tables S5 and S6 and Fig. S5 show the corresponding data for the 20/0Ni and 20/2Ni catalysts, Tables S7 and S8 and Fig. S6 show the data for 70/0Ni and 70/2Ni.

Regarding conversion, observations made in the co-oligomerization of propylene and 1-butylene are almost the same as in the homo-oligomerization of the single components. The conversion of propylene is independent of nickel loading, while the conversion of 1-butylene decreases with nickel loading. However, olefin conversion is above 80 % in both cases. Regarding the selectivity to kerosene, a decrease coming along with nickel loading is observed in the co-oligomerization too. This can be attributed again to covered Brønsted acid sites, which reduce the overall degree of oligomerization and shift the product spectrum towards shorter, less branched oligomers. The reduction of the isoindex from 2.01 to 1.95 is also related to this.

The co-oligomerization of the ternary olefin mixture, which reflects a typical MtO product mixture, exhibits no ethylene conversion without nickel on the catalyst. However, with nickel, ethylene is almost completely converted, but through ethylene dimerization, which obscures conversion of the fed 1-butylene. Without nickel, ethylene does not react in the co-oligomerization with propylene and 1-butylene and therefore, reactions of ethylene with carbenium ions of higher olefins at Brønsted acid sites can be excluded. Betz et al. [19] already pointed to this phenomenon, as in their ethylene oligomerization experiments with the same catalyst, the proportion of C_6 olefins was low compared to

Table 6
Conversions in olefin co-oligomerization over 40/0Ni and 40/2Ni (Reaction conditions: T = 120 °C, WHSV = $4h^{-1}$, $p_{Olefins}$ = 32 bar, p_{total} = 40 bar).

Catalyst	$C_3 + C_4$ co-oligomerization		$C_2 + C_3 + C_4$ co-oligomerization		
	$X_{Propylene}$ [%]	$X_{1\text{-}Butylene}$ [%]	$X_{Ethylene}$ [%]	$X_{Propylene}$ [%]	$X_{1\text{-}Butylene}$ [%]
40/0Ni	91.7	87.0	0.7	64.0	64.8
40/2Ni	91.1	81.0	95.2	87.7	62.9

Table 7
Selectivities and isoindices in olefin co-oligomerization over 40/0Ni and 40/2Ni (Reaction conditions: T = 120 °C, WHSV = 4h^{-1}, $p_{Olefins}$ = 32 bar, p_{total} = 40 bar).

Catalyst	$C_3 + C_4$ co-oligomerization			$C_2 + C_3 + C_4$ co-oligomerization		
	$S_{Gasoline}$ [%]	$S_{Kerosene}$ [%]	I_{iso} C_8	$S_{Gasoline}$ [%]	$S_{Kerosene}$ [%]	I_{iso} C_8
40/0Ni	49.9	80.1	2.01	42.0	85.5	1.97
40/2Ni	56.3	74.5	1.95	54.4	77.5	1.89

other liquid oligomers. Thus, for the co-oligomerization of ethylene, the nickel-based reaction mechanism according to Cossee-Arlman must be followed to co-oligomerize ethylene with higher olefins. The reaction mechanism is outlined in Fig. 4 for the formation of 1-hexene. As a result of ethylene conversion with nickel, the isoindex of C_8 molecules decreases to less than 1.9, which is the minimum among the results shown here.

The formation of hexenes via the nickel-based reaction pathway was already described by different research groups [77–79]. Within this study, it is evident from Fig. 5 that with nickel, the proportion of C_6 is twice as high compared to the unloaded support material. This effect is even more pronounced in the case of the catalysts 70/0Ni and 70/2Ni (Fig. S6). In contrast, data for 20/0Ni and 20/2Ni showed an opposite behavior, where the amount of C_5 and C_6 is reduced with nickel loading on the catalyst. This can be related to the overall lowest olefin conversion due to the lowest density of Brønsted acid sites of all catalysts investigated within this study.

Based on the product spectra in Fig. 5(a), it is obvious that co-oligomerization of different olefin species reduces the selectivity towards a specific carbon chain length, resulting in a much broader spectrum in the range of $C_{6\text{-}16}$. In particular, the range of $C_{7\text{-}12}$ oligomers exhibits comparable proportions. Additionally, co-oligomerization leads to higher proportions of shorter oligomers $C_{<9}$ as visible e.g. from the C_7 fraction. In this case, the reaction of propylene with butylene can lead to C_7 hydrocarbons, which ultimately reduces the yield of kerosene. Moreover, the highest share of the product distribution represented by C_{10} is most probably a co-oligomer of propylene and 1-butylene. It should be noted that the last column in the diagrams (C_{13+}) describes not only one chain length, but the range from C_{13} up to C_{18} and furthermore distorts the product distribution regarding longer carbon chain lengths. In conclusion, co-oligomerization and homo-oligomerization reactions take place to a comparable extent and thus, there is no pre-determined reaction pathway for the (co–)oligomerization reactions via specific intermediates.

Without nickel, ethylene from the MtO surrogate does not react, indicating a co-oligomerization of C_3 and C_4. In this process, the partial pressure of propylene (12.8 bar) is twice as high as the one of 1-butylene (6.4 bar), and the inert component consists of 52 % ethylene in addition to 20 % argon. These differences affect the product spectrum (Fig. 5(b)), resulting in a significantly higher proportion of long-chain oligomers in the C_{13+} chain length range compared to the equimolar oligomerization of propylene and 1-butylene (Fig. 5(a)).

When nickel is present, the fraction of long-chain oligomers in the C_{13+} range decreases again. The product spectrum shifts towards shorter oligomers, which is evident from the diagram, particularly regarding the $C_{7\text{-}11}$ chain length range. Thus, observations from the homo-oligomerization experiments are entirely in accordance with those from the co-oligomerization of olefin mixtures.

3.2.2. *Co-oligomerization of $C_2 + C_3 + C_4$ olefin mixtures in a two-bed reactor*

As described before, the nickel-catalyzed oligomerization results in lower fuel qualities in terms of lower cold flow properties, knocking resistances and reduced yields of kerosene. As at comparatively low temperatures ethylene requires nickel sites for the oligomerization, experiments with two catalysts in series were conducted. In this set-up the first one is loaded with a catalyst containing nickel to mainly convert ethylene to butylenes and hexenes. The conversion of propylene and butylenes is reduced to a minimum by using a carrier with low Brønsted acidity and thus, 20/2Ni was chosen. The second catalyst is free of nickel and provides a high density of Brønsted acid sites (40/0Ni) for the acid catalyzed oligomerization of C_{3+} olefins to highly branched oligomers in the range of kerosene. The proportions of the catalysts are 2.5 g each, aligned in series to maintain an overall catalyst mass of 5 g.

The results of the experiments conducted with the combined catalysts 20/2Ni and 40/0Ni are summarized in the following. Due to the reduced amount of nickel sites, ethylene conversion is slightly reduced, but propylene and butylene conversion raise significantly due to the higher amount of Brønsted acid sites deployed by 40/0Ni (Table 8). For 20/2Ni it should be mentioned that the negative conversion of butylene results from the high selectivity of ethylene oligomerization to butylene and the low conversion of the initial fed butylenes due to the low density of Brønsted acid sites of the catalyst. Compared to the experiments solely with 20/2Ni, the combination of the two catalysts in series reveals the targeted increase in branching as shown by the isoindex raising from 1.75 to 1.97 (Table 9). Selectivity to kerosene also increases due to a shift in the product distribution to longer oligomers, which is best visible for C_{12} and C_{13+} (Fig. 6). The shift is related to the elevated availability of acid sites for the oligomerization of C_{3+} olefins in the lower part of the reactor provided by 40/0Ni and promoting the formation of kerosene. In the Supplementary Information the results for the catalyst combinations 40/2Ni + 40/0Ni as well as 70/2Ni + 40/0Ni are shown in Chapter S5 revealing the same effects described for 20/2Ni and 40/0Ni.

3.2.3. *Reaction networks*

An overview on possible oligomerization reactions of ethylene, propylene and butylenes to oligomers with carbon chain lengths of up to C_{12} is shown in Fig. 7. The thick arrows represent the oligomerization pathways of ethylene, propylene and butylene to their integer multiples. The thinner arrows show the possible co-oligomerization reactions. For clarity reasons, C_{12} was chosen as longest oligomer, but longer oligomers in the range of kerosene are formed according to the same mechanisms. Additionally, (co–)oligomerizations of higher olefins, e.g. the reaction of C_4 with C_5 to form C_9 or the dimerization of C_6 to form C_{12}, are omitted. Furthermore, side reactions like metathesis are not depicted as they have little impact. Regarding the occuring secondary reactions, Toch et al. developed a scheme starting with ethylene dimerization at nickel sites and a focus on subsequent acid site catalyzed reactions [20].

As can be seen, several co-oligomerization routes are possible, and

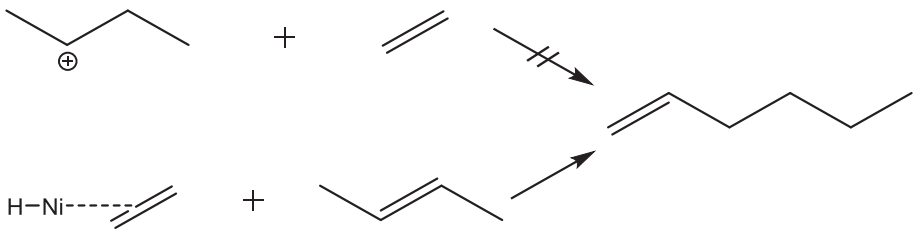

Fig. 4. Reaction pathway for 1-hexene formation from ethylene and butylene at T = 120 °C.

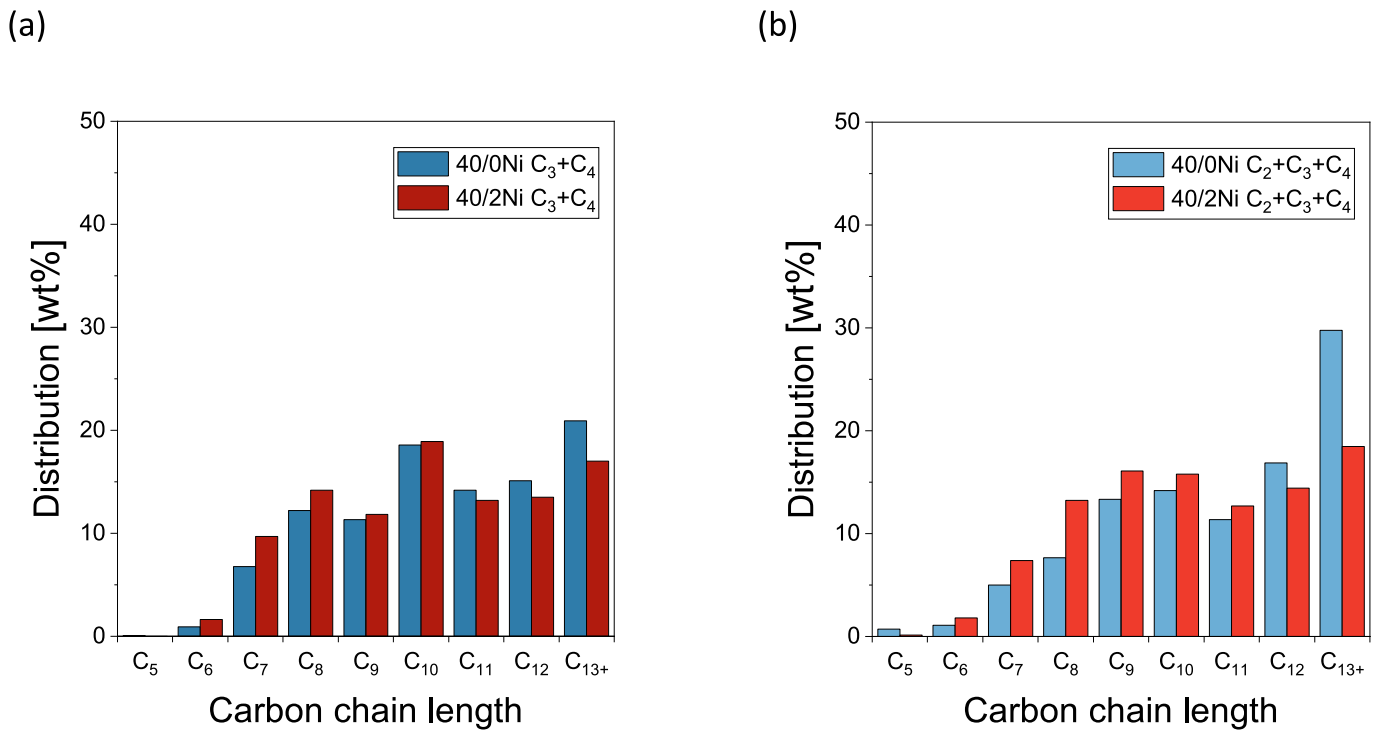

Fig. 5. Product distribution of (a) $C_3 + C_4$ and (b) $C_2 + C_3 + C_4$ co-oligomerization over 40/0Ni and 40/2Ni (Reaction conditions: T = 120 °C, WHSV = $4h^{-1}$, $p_{Olefins}$ = 32 bar, p_{total} = 40 bar).

Table 8
Conversions in olefin co-oligomerization over 20/2Ni and 20/2Ni + 40/0Ni (Reaction conditions: T = 120 °C, WHSV = $4h^{-1}$, $p_{Olefins}$ = 32 bar, p_{total} = 40 bar).

Catalyst	$X_{Ethylene}$ [%]	$X_{Propylene}$ [%]	$X_{1\text{-}Butylene}$ [%]
20/2Ni	35.0	21.7	−0.7
20/2Ni + 40/0Ni	27.4	64.6	59.7

Table 9
Selectivities and isoindices in olefin co-oligomerization over 20/2Ni and 20/2Ni + 40/0Ni (Reaction conditions: T = 120 °C, WHSV = $4h^{-1}$, $p_{Olefins}$ = 32 bar, p_{total} = 40 bar).

Catalyst	$S_{Gasoline}$ [%]	$S_{Kerosene}$ [%]	I_{iso} C_8
20/2Ni	65.7	72.6	1.75
20/2Ni + 40/0Ni	46.9	81.0	1.97

the spectrum of oligomers with varying carbon chain lengths extends throughout the displayed range and even beyond to longer chains. Based on the previously depicted product distributions, it is evident that pentenes and hexenes are present in comparatively small proportions while higher oligomers are dominating. This suggests that the formed C_5 and C_6 oligomers are only intermediates and quickly react further to form larger molecules.

Since the reaction of ethylene without nickel can be ruled out under the given reaction conditions, the reaction network from Fig. 7 can be simplified for this case. All reactions involving ethylene that require a nickel catalyst represented by grey arrows can be removed. Additionally, the reaction of propylene with ethylene to form pentenes is excluded, so that pentenes do not originate from oligomerization reactions and are exclusively formed through metathesis reactions. The resulting simplified reaction network for a nickel-free catalyst is shown in Fig. 8. Based on this scheme, simplified kinetic models and simulations can be created in further studies due to the reduced number of

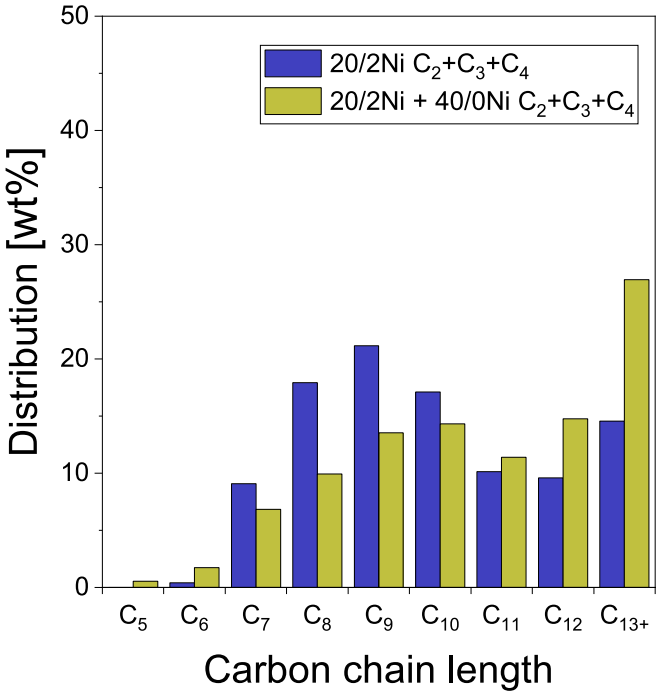

Fig. 6. Product distribution of $C_2 + C_3 + C_4$ co-oligomerization over 20/2Ni and 20/2Ni + 40/0Ni (Reaction conditions: T = 120 °C, WHSV = $4h^{-1}$, $p_{Olefins}$ = 32 bar, p_{total} = 40 bar).

olefin species and oligomerization reactions. By this, chain length distributions and the associated fuel properties could be predicted.

3.2.4. *Long-term experiment*

A long-term experiment employing the MtO surrogate, i.e. a mixture of 40 mol% ethylene, 40 mol% propylene and 20 mol% 1-butylene, was

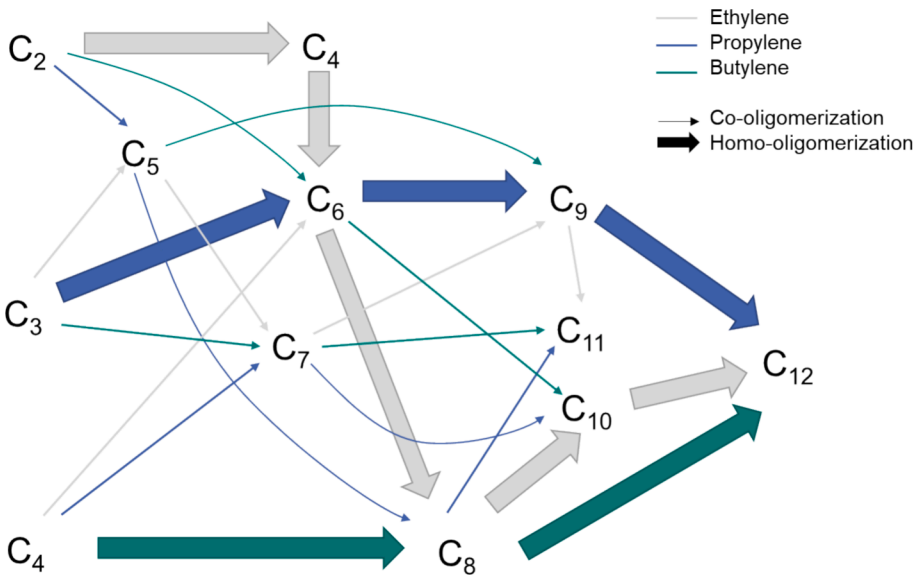

Fig. 7. Reaction network of the (co–)oligomerization of C_{2-4} olefins up to carbon chain lengths of C_{12}.

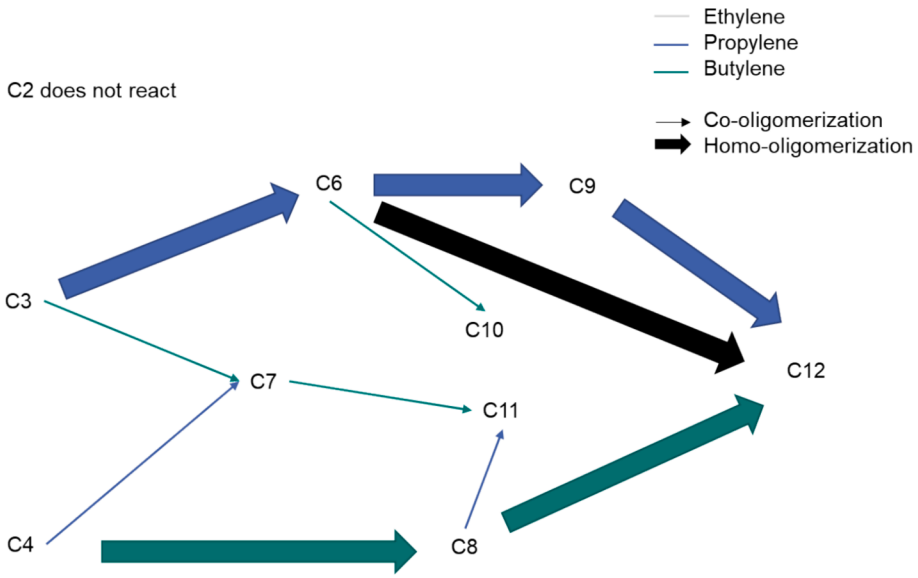

Fig. 8. Simplified reaction network of the (co–)oligomerization of a C_{2-4} olefin mixture without nickel-catalyzed oligomerization reactions of ethylene.

conducted. The objective was twofold: firstly, to evaluate the stability of the catalysts and secondly, to generate a sufficient fuel quantity for an analysis of fuel properties. For this purpose, the nickel-loaded catalyst 40/2Ni was used, which converts all olefin species at a temperature of 120 °C, an olefin partial pressure of 32 bar, a total pressure of 40 bar and a WHSV of 4 h^{-1}.

The experiment was run with a time on stream (TOS) of 222 h yielding a total of 3.8 L of fuel. Fig. 9 illustrates the progress of the conversion of the supplied olefins. However, 1-butylene conversion is again obscured by the dimerization of ethylene to form butylenes. Ethylene conversion stays above 95 %, while the conversion of propylene and 1-butylene decreases over TOS. This is due to blocking of the acid sites by deposits of longer oligomers not desorbing from the catalyst. It is also visible, that the decrease of 1-butylene conversion is faster than for propylene. Another reason for this is the formation of butylenes by increased ethylene dimerization. This effect gets more pronounced as fewer acid sites for the oligomerization of higher olefins are available, so consequently, the oligomerization of the produced butylenes is slowing down over TOS. As a result, the measured conversion of 1-butylene decreases.

Ethylene oligomerization is not significantly decreasing, although accessibility of nickel sites should also be reduced. This indicates an excess of nickel sites and even with a deactivated 40/2Ni catalyst, sufficient nickel sites are available for ethylene oligomerization. After 102 h TOS, the catalyst was regenerated at ambient pressure and 300 °C under an argon flow of 200 ml/min to remove soft coke from the catalyst surface. Formation of soft coke in oligomerization reactions was already described by Diaz et al. [39]. After regeneration, at 126 h TOS, conversion of C_3 and C_4 was remarkably higher, but did not reach the initial value. Consequently, hard coke has probably been formed on the catalyst, which is blocking acid sites [29,39]. The removal of hard coke may be conducted by burning it off with air as it is done on industrial scale. However, on lab-scale this is not applicable. It is also visible, that after 200 h TOS almost constant olefin conversion was reached, even for propylene and 1-butylene. Thus, the co-oligomerization seems to reach a pseudo-steady state.

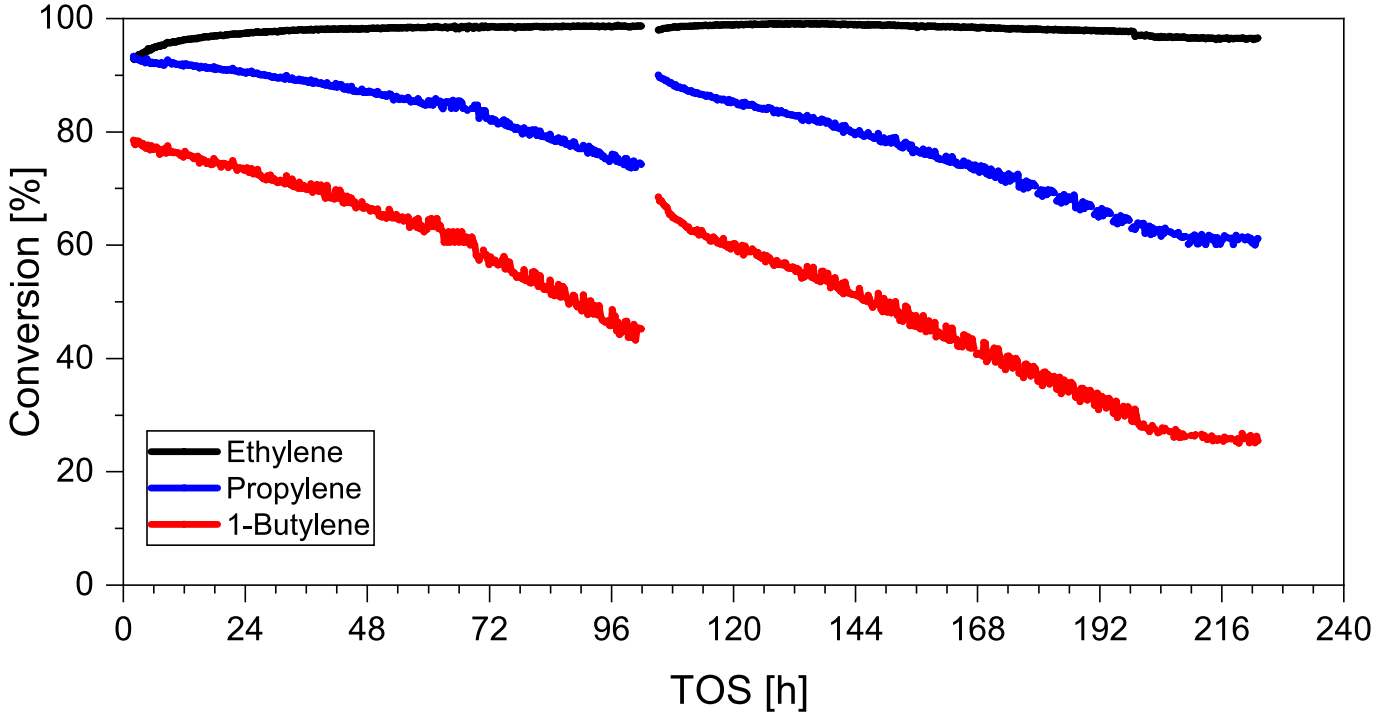

Fig. 9. Conversion of ethylene, propylene and 1-butylene with catalyst 40/2Ni as a function of TOS (Reaction conditions: T = 120 °C, WHSV = $4h^{-1}$, $p_{Olefins}$ = 32 bar, p_{total} = 40 bar).

Fig. 10 presents the evolution of the product composition at different TOS during the experiment, as well as the composition of the overall collected product (black column). In the initial phase, a selectivity to kerosene of more than 77 wt% was achieved, after 222 h it decreased to 47 wt%. Regarding the total amount of liquid products, kerosene ultimately accounts for 63 wt%. This trend towards shorter chain length with increasing TOS is most evident for the C_{13+} fraction. Once again, this effect is related to the blocking of acid sites, impeding the consecutive oligomerization of higher olefins. As in the case of olefin conversion (Fig. 9), catalyst regeneration did not lead to a complete recovery of the initial performance.

3.2.5. *Fuel properties*

Fig. 11 displays the isoindex as a function of TOS, revealing that the Brønsted acid sites become blocked in the course of the experiment, leading to a decrease in isomerization reactions. The isoindex of the total product is 1.79. Similar to the previously shown effects on conversion and product distribution, the regeneration after 102 h TOS does not recover the initial performance. Consequently, the isoindex rises immediately after regeneration, but after another 50 h TOS, the degree of branching is on the same level as before regeneration. Until the end of the experiment, the isoindex decreases steadily to 1.63 due to the further deposition of longer-chain oligomers on acid sites.

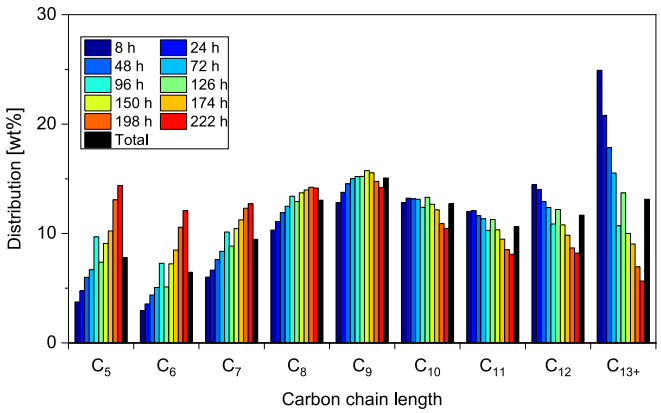

Fig. 10. Development of the chain length distribution with TOS and overall product composition (Reaction conditions: T = 120 °C, WHSV = $4h^{-1}$, $p_{Olefins}$ = 32 bar, p_{total} = 40 bar).

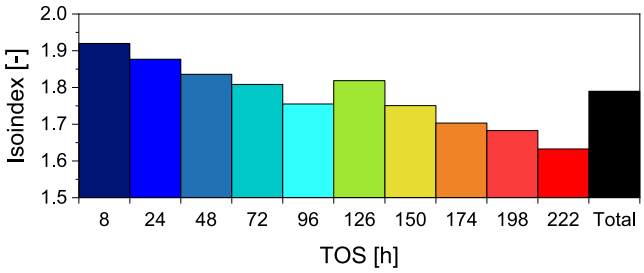

Fig. 11. Isoindex as a function of TOS and composition of the overall liquid product (Reaction conditions: T = 120 °C, WHSV = $4h^{-1}$, $p_{Olefins}$ = 32 bar, p_{total} = 40 bar).

No hydrogenation of the product mixtures was carried out and the olefin mixtures were analyzed directly, to get a first impression of the fuel quality. Afterwards, possible efforts for further refinement and properties of the corresponding paraffins can be estimated with reasonable accuracy.

The produced liquid oligomers up to a TOS of 200 h were taken into account and the fractions were separated by destillation. For the gasoline fraction, the fraction up to a boiler temperature of 210 °C was utilized, while the whole fraction with a boiler temperature above 150 °C was applied for kerosene analysis. The corresponding chain length distributions are depicted in Fig. 12.

In Table 10, the analyzed parameters of the kerosene fraction according to the corresponding analysis standards are shown. Many parameters comply with the standard. The density is slightly below the requirement, but it can be easily adjusted by blending. The freezing

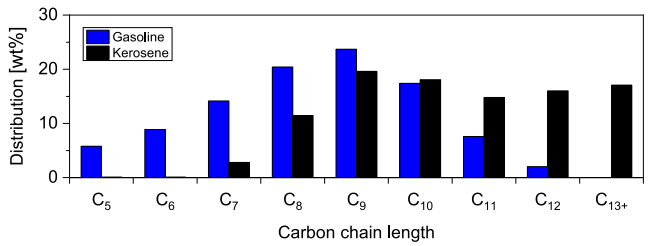

Fig. 12. Compositions of the gasoline and kerosene fractions.

Table 10
Properties of the oligomeric kerosene fraction.

Property	Unit	Oligomeric kerosene	Requirement of ASTM D7566
Acid number	mg KOH/g	0.034	Max. 0.1
Density at 15 °C	kg/m^3	773.2	775—840
Flash point	°C	<40	Min. 38
Freezing point	°C	−38.2	Max. −47 (Jet A-1) Max. −40 (Jet A)
Viscosity at −20 °C	mm^2/s	2.940	Max. 8
Net heat of combustion	MJ/kg	43.328	Min. 42.8
Smoke point	mm	24.7	Min. 25
Distillation:			
Boiling start	°C	132.1	–
Final boiling point	°C	304.1	300
10 %-Point	°C	143.0	205
50 %-Point	°C	170.5	–
90 %-Point	°C	244.9	–

point is at −38.2 °C and thus, it is not sufficiently low. This correlates with the high final boiling point of 304.1 °C. Since the whole fraction above a boiler temperature of 150 °C was assigned to the kerosene fraction, it also contains oligomers in the range of diesel fuel. Separating the fraction with a boiling point above 250 °C will slightly reduce the yield of the kerosene fraction as can be seen from the 90 % value of the distillation, but the fuel quality will increase in terms of a lower freezing temperature.

The properties of the oligomeric gasoline fraction are specified in Table 11. The fuel meets the standard regarding research octane number (RON) and density. The high RON results from the high share of branched olefins. The vapor pressure is too low due to a low share of short chain oligomers. Consequently, below 130 °C the fuel evaporates slower than required according to DIN EN228. On the other hand, at 161.3 °C already 90 % is evaporated and the final boiling point of 183.4 °C is standard compliant. By blending, boiling can be shifted to the required area. It is to mention, that the standard allows for 18 vol% of olefins, so this oligomeric gasoline has to be blended anyway. By hydrogenation of the oligomers, higher blending shares are possible but the RON decreases, since paraffins usually lead to lower RON compared to the corresponding olefins.

Table 11
Properties of the oligomeric gasoline fraction.

Property	Unit	Oligomeric gasoline	Requirement of DIN EN228
Research octane number (RON)	–	95.2	95
Density at 15 °C	kg/m^3	735.5	720—775
Vapor pressure DVPE	kPa	21.5	45—90
Net heat of combustion	MJ/kg	41.773	–
Distillation:			
Boiling start	°C	54.9	< 210
Final boiling point	°C	183.4	–
10 %-Point	°C	92.8	–
50 %-Point	°C	131.2	–
90 %-Point	°C	161.3	–
Distillation residue	vol%	1.0	<2

4. Conclusions

(Co–)Oligomerization of olefins represents a promising pathway for the synthesis of sustainable kerosene. This study demonstrates that short-chain olefins in the $C_{2\text{-}4}$ range can be converted to kerosene with conversions and selectivities exceeding 90 %. Regarding the homo-oligomerization of propylene and 1-butylene, the influence of space velocity on the product spectrum was investigated in detail. It was found that due to the stabilization of carbenium ions by larger + I-effects of substituting alkyl groups, 1-butylene exhibits higher reactivity than propylene. A WHSV of 4 h^{-1} proved to be advantageous for synthesizing oligomers in the kerosene range.

In addition to olefin homo-oligomerization, the impact of the olefin feed on the product spectrum was investigated for the co-oligomerization of propylene and 1-butylene, and for the co-oligomerization of a MtO surrogate, i.e. a typical olefin mixture obtainable by the conversion of methanol and comprising ethylene, propylene as well as 1-butylene. With an increasing number of possible oligomerization pathways, a broad product spectrum emerges with reduced selectivity towards specific carbon chain lengths compared to homo-oligomerization. However, a selectivity towards kerosene of above 80 % is still achievable.

It has been demonstrated that for ethylene oligomerization and co-oligomerization under mild conditions, the presence of a transition metal like nickel is essential for the reaction to occur. However, in the case of nickel catalysts, molecular branching of the resulting oligomers decreases, slightly compromising cold flow properties. For the byproduct gasoline, fuel-relevant properties also deteriorate, which manifests itself especially in the form of lower octane ratings. Without nickel, the reaction of ethylene with carbenium ions of the olefins does not take place. Therefore, the activation of ethylene is initially necessary before it can react with another olefin. Consequently, in the context of the co-oligomerization reaction network of ethylene with propylene and butylenes, the absence of nickel significantly simplifies it to a selective co-oligomerization of propylene and butylene with the benefit of a higher selectivity to kerosene. Applying a catalyst bed consisting of two different catalysts, a nickel-loaded catalyst with moderate acidity and a nickel-free catalyst with higher acidity in series, allows for the compensation of the negative effects coming along with ethylene oligomerization at nickel sites. In addition to higher degrees of branching, fuel quality and kerosene yield increase to values comparable to those achieved with nickel-free catalysts.

Finally, stability of the catalyst 40/2Ni was investigated in a long-term experiment lasting for 222 h TOS. The co-oligomerization of a typical MtO surrogate initially exhibited a high selectivity to kerosene of 77 %. However, with increasing TOS and progressive catalyst deactivation, the product spectrum shifted towards shorter chains in the gasoline range. As a result, the selectivity to kerosene decreased over time and amounts to 63 % of the total product. The analysis of physicochemical properties revealed that the synthesized kerosene fraction complies with many properties of the ASTM D7566 standard. Hydrogenation and blending with commercial kerosene after separating the remaining diesel fuel fraction can help to entirely meet the standard. Thus, it has been proven that the co-oligomerization of short-chain olefins under mild reaction conditions produces kerosene with high yields, potentially playing a significant role in the large-scale synthesis of synthetic paraffinic kerosene in the future.

CRediT authorship contribution statement

Constantin Fuchs: Writing – original draft, Methodology, Investigation, Formal analysis, Data curation. **Ulrich Arnold:** Writing – review & editing, Supervision, Project administration, Investigation, Funding acquisition, Conceptualization. **Jörg Sauer:** Writing – review & editing, Supervision, Project administration, Conceptualization.

Declaration of competing interest

The authors declare that they have no known competing financial interests or personal relationships that could have appeared to influence the work reported in this paper.

Acknowledgments

The authors gratefully acknowledge financial support from the Baden-Württemberg Ministry of Transport and the "Strategiedialog Automobilwirtschaft BW" within the project "reFuels – Rethinking Fuels''. Financial support from the Bundesministerium für Digitales und Verkehr (BMDV) / Fachagentur Nachwachsende Rohstoffe (FNR), Germany, within the joint research project "Renewable Fuels from Green Refineries of the Future" (FKZ: 16RK24001B) is also gratefully acknowledged. The authors thank Sasol for providing catalyst materials and the Leibniz Institute for Catalysis (LIKAT) for conducting pyridine-DRIFTS measurements.

Appendix A. Supplementary material

Supplementary data to this article can be found online at https://doi.org/10.1016/j.fuel.2024.133680.

Data availability

Data will be made available on request.

References

[1] Kramer S, Andac G, Heyne J, Ellsworth J, Herzig P, Lewis KC. Perspectives on fully synthesized sustainable aviation fuels. Direction and Opportunities Front Energy Res 2022;9. https://doi.org/10.3389/fenrg.2021.782823.
[2] Holladay J, Abdullah Z, Heyne J. Sustainable aviation fuel: review of technical. Pathways 2020.
[3] Grimme W. The introduction of sustainable aviation fuels—a discussion of challenges, options and alternatives. Aerospace 2023;10(3). https://doi.org/10.3390/aerospace10030218.
[4] Wang W-C, Tao L. Bio-jet fuel conversion technologies. Renew Sustain Energy Rev 2016;53:801–22. https://doi.org/10.1016/j.rser.2015.09.016.
[5] Cabrera E, de Sousa JMM. Use of sustainable fuels in aviation—a review. Energies 2022;15(7). https://doi.org/10.3390/en15072440.
[6] Dry ME. The Fischer-Tropsch (FT) Synthesis Processes. In: Ertl G, editor. Handbook of heterogeneous catalysis 2. Ed. Weinheim, Chichester: Wiley-VCH; 2008.
[7] Eagan NM, Kumbhalkar MD, Buchanan JS, Dumesic JA, Huber GW. Chemistries and processes for the conversion of ethanol into middle-distillate fuels. Nat Rev Chem 2019;3(4):223–49. https://doi.org/10.1038/s41570-019-0084-4.
[8] Pechstein J, Neuling U, Gebauer J, Kaltschmitt M. Alcohol-to-Jet (AtJ). In: Kaltschmitt M, Neuling U, editors. Biokerosene. Heidelberg: Springer, Berlin Heidelberg, Berlin; 2018. p. 543–74.
[9] Kurzawska P. Overview of sustainable aviation fuels including emission of particulate matter and harmful gaseous exhaust gas compounds. Transp Res Procedia 2021;59:38–45. https://doi.org/10.1016/j.trpro.2021.11.095.
[10] European Union Aviation Safety Agency. Updated analysis of the non-CO_2 climate impacts of aviation and potential policy measures pursuant to EU Emissions Trading System Directive Article 30(4). 2020.
[11] Meurer A, Kern J. Fischer-Tropsch synthesis as the key for decentralized sustainable kerosene production. Energies 2021;14(7):1836. https://doi.org/10.3390/en14071836.
[12] Ail SS, Dasappa S. Biomass to liquid transportation fuel via Fischer Tropsch synthesis – technology review and current scenario. Renew Sustain Energy Rev 2016;58:267–86. https://doi.org/10.1016/j.rser.2015.12.143.
[13] Fuchs C, Arnold U, Sauer J. (Co-)Oligomerization of olefins to hydrocarbon fuels: influence of feed composition and pressure. Chem Ing Tech 2023;95(5):651–7. https://doi.org/10.1002/cite.202200209.
[14] Olsbye U, Svelle S, Bjørgen M, Beato P, Janssens TVW, Joensen F, et al. Conversion of methanol to hydrocarbons: how zeolite cavity and pore size controls product selectivity. Angew Chem Int Ed Engl 2012;51(24):5810–31. https://doi.org/10.1002/anie.201103657.
[15] Stöcker M. Methanol to Olefins (MTO) and Methanol to Gasoline (MTG). In: Cejka J, Corma A, Zones S, editors. Zeolites and catalysis. Synthesis, reactions and applications. [John Wiley, distributor], Weinheim, [Chichester]: Wiley-VCH; 2010. p. 687–711.
[16] Niethammer B, Arnold U, Sauer J. Suppressing the aromatic cycle of the dimethyl ether to hydrocarbons reaction on zeolites. Appl Catal A 2023;651:119021. https://doi.org/10.1016/j.apcata.2023.119021.
[17] O'Connor CT. Oligomerization. In: Ertl G, editor. Handbook of heterogeneous catalysis 2. Ed. Weinheim, Chichester: Wiley-VCH; 2008.
[18] Koninckx E, Mendes PS, Thybaut JW, Broadbelt LJ. Ethylene oligomerization on nickel catalysts on a solid acid support: from New mechanistic insights to tunable bifunctionality. Appl Catal A 2021;624:118296. https://doi.org/10.1016/j.apcata.2021.118296.
[19] Betz M, Fuchs C, Zevaco TA, Arnold U, Sauer J. Production of hydrocarbon fuels by heterogeneously catalyzed oligomerization of ethylene: tuning of the product distribution. Biomass Bioenergy 2022;166:106595. https://doi.org/10.1016/j.biombioe.2022.106595.
[20] Toch K, Thybaut JW, Arribas MA, Martínez A, Marin GB. Steering linear 1-alkene, propene or gasoline yields in ethene oligomerization via the interplay between nickel and acid sites. Chem Eng Sci 2017;173:49–59. https://doi.org/10.1016/j.ces.2017.07.025.
[21] Nicholas CP. Applications of light olefin oligomerization to the production of fuels and chemicals. Appl Catal A 2017;543:82–97. https://doi.org/10.1016/j.apcata.2017.06.011.
[22] Olivier-Bourbigou H, Breuil PAR, Magna L, Michel T, Espada Pastor MF, Delcroix D. Nickel catalyzed olefin oligomerization and dimerization. Chem Rev 2020;120(15):7919–83. https://doi.org/10.1021/acs.chemrev.0c00076.
[23] Brogaard RY, Olsbye U. Ethene oligomerization in Ni-containing zeolites: theoretical discrimination of reaction mechanisms. ACS Catal 2016;6(2):1205–14. https://doi.org/10.1021/acscatal.5b01957.
[24] Forget S, Olivier-Bourbigou H, Delcroix D. Homogeneous and heterogeneous nickel-catalyzed olefin oligomerization: experimental investigation for a common mechanistic proposition and catalyst optimization. ChemCatChem 2017;9(12):2408–17. https://doi.org/10.1002/cctc.201700348.
[25] Finiels A, Fajula F, Hulea V. Nickel-based solid catalysts for ethylene oligomerization – a review. Cat Sci Technol 2014;4(8):2412–26. https://doi.org/10.1039/C4CY00305E.
[26] Fuchs C, Arnold U, Sauer J. Effect of nickel loading on fuel production via heterogeneously catalyzed oligomerization of methanol-based olefins. Chem Ing Tech 2022;94(9):1215. https://doi.org/10.1002/cite.202255176.
[27] Corma A, Martínez C, Doskocil E. Designing MFI-based catalysts with improved catalyst life for $C_{3=}$ and $C_{5=}$ oligomerization to high-quality liquid fuels. J Catal 2013;300:183–96. https://doi.org/10.1016/j.jcat.2012.12.029.
[28] Li X, Han D, Wang H, Liu G, Wang B, Li Z, et al. Propene oligomerization to high-quality liquid fuels over Ni/HZSM-5. Fuel 2015;144:9–14. https://doi.org/10.1016/j.fuel.2014.12.005.
[29] Flego C, Peratello S, Peregoe C, Sabatino LMF, Belussi G, Romano U. Reaction and deactivation study of mesoporous silica–alumina (MSA) in propene oligomerisation. J Mol Catal A Chem 2003;204–205(581–589). https://doi.org/10.1016/S1381-1169(03)00341-8.
[30] Spinicci R, Tofanari A. A study of the propylene oligomerization on silica-alumina supported nickel oxide. Mater Chem Phys 1990;25(4):375–83. https://doi.org/10.1016/0254-0584(90)90126-U.
[31] Zhang J, Yan Y, Chu Q, Feng J. Solid phosphoric acid catalyst for propene oligomerization: effect of silicon phosphate composition. Fuel Process Technol 2015;135:2–5. https://doi.org/10.1016/j.fuproc.2014.09.007.
[32] Mlinar AN, Shylesh S, Ho OC, Bell AT. Propene oligomerization using alkali metal- and nickel-exchanged mesoporous aluminosilicate catalysts. ACS Catal 2014;4(1):337–43. https://doi.org/10.1021/cs4007809.
[33] Mlinar AN, Zimmerman PM, Celik FE, Head-Gordon M, Bell AT. Effects of Brønsted-acid site proximity on the oligomerization of propene in H-MFI. J Catal 2012;288:65–73. https://doi.org/10.1016/j.jcat.2012.01.002.
[34] Deimund MA, Labinger J, Davis ME. Nickel-exchanged zincosilicate catalysts for the oligomerization of propylene. ACS Catal 2014;4(11):4189–95. https://doi.org/10.1021/cs501313z.
[35] Vernuccio S, Bickel EE, Gounder R, Broadbelt LJ. Microkinetic model of propylene oligomerization on brønsted acidic zeolites at low conversion. ACS Catal 2019;9(10):8996–9008. https://doi.org/10.1021/acscatal.9b02066.
[36] Vaughan JS, O'Connor CT, Fletcher J. High-pressure oligomerization of propene over heteropoly acids. J Catal 1994;147(2):441–54. https://doi.org/10.1006/jcat.1994.1161.
[37] Albrecht S, Kießling D, Wendt G, Maschmeyer D, Nierlich F. Oligomerisierung von n-Butenen. Chem Ing Tech 2005;77(6):695–709. https://doi.org/10.1002/cite.200407090.
[38] Díaz M, Epelde E, Tabernilla Z, Ateka A, Aguayo AT, Bilbao J. Operating conditions to maximize clean liquid fuels yield by oligomerization of 1-butene on HZSM-5 zeolite catalysts. Energy 2020;207:118317. https://doi.org/10.1016/j.energy.2020.118317.
[39] Díaz M, Epelde E, Valecillos J, Izaddoust S, Aguayo AT, Bilbao J. Coke deactivation and regeneration of HZSM-5 zeolite catalysts in the oligomerization of 1-butene. Appl Catal B 2021;291:120076. https://doi.org/10.1016/j.apcatb.2021.120076.

[40] Nadolny F, Alscher F, Peitz S, Borovinskaya E, Franke R, Reschetilowski W. Influence of remaining acid sites of an amorphous aluminosilicate on the oligomerization of n-butenes after impregnation with nickel ions. Catalysts 2020; 10(12):1487. https://doi.org/10.3390/catal10121487.
[41] Silva AF, Fernandes A, Antunes MM, Neves P, Rocha SM, Ribeiro MF, et al. TUD-1 type aluminosilicate acid catalysts for 1-butene oligomerisation. Fuel 2017;209: 371–82. https://doi.org/10.1016/j.fuel.2017.08.017.
[42] Silva AF, Fernandes A, Neves P, Antunes MM, Rocha SM, Ribeiro MF, et al. Mesostructured catalysts based on the BEA topology for olefin oligomerisation. ChemCatChem 2018;10(13):2741–54. https://doi.org/10.1002/cctc.201701597.
[43] Cossee PJ. Ziegler-natta catalysis I. Mechanism of polymerization of alpha;-olefins with Ziegler-Natta catalysts. J Catal 1964;3(1):80–8. https://doi.org/10.1016/0021-9517(64)90095-8.
[44] Shao H, Li H, Lin J, Jiang T, Guo X, Li J. Metallocene-catalyzed oligomerizations of 1-butene and α-olefins: toward synthetic lubricants. Eur Polym J 2014;59:208–17. https://doi.org/10.1016/j.eurpolymj.2014.08.002.
[45] Ehrmaier A, Liu Y, Peitz S, Jentys A, Chin Y-H-C, Sanchez-Sanchez M, et al. Dimerization of linear Butenes on zeolite-supported Ni 2+. ACS Catal 2019;9(1): 315–24. https://doi.org/10.1021/acscatal.8b03095.
[46] McGuinness DS. Olefin oligomerization via metallacycles: dimerization, trimerization, tetramerization, and beyond. Chem Rev 2011;111(3):2321–41. https://doi.org/10.1021/cr100217q.
[47] D02 Committee. Specification for Aviation Turbine Fuels. ASTM International, West Conshohocken, PA. https://doi.org/10.1520/D1655-20D.
[48] Grudanova AI, Gulyaeva LA, Krasilnikova LA, Shmelkova OI, Boldushevskii RE. Jet fuel and arctic diesel fuel production by isodewaxing of waxy middle distillate fractions. Fuel 2017;193:485–7. https://doi.org/10.1016/j.fuel.2016.12.032.
[49] Lallemand M, Finiels A, Fajula F, Hulea V. Nature of the Active sites in ethylene oligomerization catalyzed by Ni-containing molecular sieves: chemical and IR spectral investigation. J Phys Chem C 2009;113(47):20360–4. https://doi.org/10.1021/jp9082932.
[50] American Petroleum Institute. 1958. Knocking Characteristics of Pure Hydrocarbons. ASTM International.
[51] Ahoba-Sam C, Erichsen MW, Olsbye U. Ethene and butene oligomerization over isostructural H-SAPO-5 and H-SSZ-24: Kinetics and mechanism. Chin J Catal 2019; 40(11):1766–77. https://doi.org/10.1016/S1872-2067(19)63426-1.
[52] Antunes BM, Rodrigues AE, Lin Z, Portugal I, Silva CM. Alkenes oligomerization with resin catalysts. Fuel Process Technol 2015;138:86–99. https://doi.org/10.1016/j.fuproc.2015.04.031.
[53] Liu P, Redekop E, Gao X, Liu W-C, Olsbye U, Somorjai GA. Oligomerization of light olefins catalyzed by brønsted-acidic metal-organic framework-808. J Am Chem Soc 2019;141(29):11557–64. https://doi.org/10.1021/jacs.9b03867.
[54] Ipatieff VN, Corson BB, Egloff G. Polymerization, a new source of gasoline. Ind Eng Chem 1935;27(9):1077–81. https://doi.org/10.1021/ie50309a027.
[55] Babu BH, Lee M, Hwang DW, Kim Y, Chae H-J. An integrated process for production of jet-fuel range olefins from ethylene using Ni-AlSBA-15 and Amberlyst-35 catalysts. Appl Catal A 2017;530:48–55. https://doi.org/10.1016/j.apcata.2016.11.020.
[56] Kriván E, Tomasek S, Hancsók J. The oligomerization of high olefin containing hydrocarbon by-products to clean engine fuels. J Clean Prod 2016;136:81–8. https://doi.org/10.1016/j.jclepro.2016.06.020.
[57] M. Peters, J. Taylor. 2011. Renewable jet fuel blendstock from isobutanol. World Patent (WO 2011/140560).
[58] Tabak SA, Yurchak S. Conversion of methanol over ZSM-5 to fuels and chemicals. Catal Today 1990;6(3):307–27. https://doi.org/10.1016/0920-5861(90)85007-b.
[59] Tabak SA, Krambeck FJ. Shaping process makes fuels hydrocarbon process. (United States) 1985;64(9):72–4.
[60] York D, Scheckler J, Tajbl D. UOP catalytic Condensation Process For Transportation Fuels. In: Meyers RA, editor. Handbook of Petroleum Refining Processes. Chapter: McGraw-Hill; 1997. p. 1–3.
[61] Tian P, Wei Y, Ye M, Liu Z. Methanol to Olefins (MTO): from fundamentals to commercialization. ACS Catal 2015;5(3):1922–38. https://doi.org/10.1021/acscatal.5b00007.
[62] Gogate MR. Methanol-to-olefins process technology: current status and future prospects. Pet Sci Technol 2019;37(5):559–65. https://doi.org/10.1080/10916466.2018.1555589.
[63] Boltz M, Losch P, Louis B. A general overview on the methanol to olefins reaction: recent catalyst developments. Adv Chem Lett 2013;1(3):247–56. https://doi.org/10.1166/acl.2013.1032.
[64] Keil FJ. Methanol-to-hydrocarbons: process technology. Microporous Mesoporous Mater 1999;29(1–2):49–66. https://doi.org/10.1016/S1387-1811(98)00320-5.
[65] Heveling J, Nicolaides CP, Scurrell MS. Catalysts and conditions for the highly efficient, selective and stable heterogeneous oligomerisation of ethylene. Appl Catal A 1998;173(1):1–9. https://doi.org/10.1016/S0926-860X(98)00147-1.
[66] Dagle VL, Affandy M, Lopez JS, Cosimbescu L, Gaspar DJ, Scott Goldsborough S, et al. Production, fuel properties and combustion testing of an iso-olefins blendstock for modern vehicles. Fuel 2022;310(122314). https://doi.org/10.1016/j.fuel.2021.122314.
[67] Pines H. The Chemistry of Catalytic Hydrocarbon Conversions. Acid-Catalyzed Reactions: Elsevier, Academic Press, London; 1981.
[68] Lossing FP, Semeluk GP. Free radicals by mass spectrometry. XLIL Ionization potentials and ionic heats of formation for C 1 —C 4 alkyl radicals. Can J Chem 1970;48(6):955–65. https://doi.org/10.1139/v70-157.
[69] Lukyanov DB. Reactivity of propene, n-Butene, and isobutene in the hydrogen transfer steps of n-hexane cracking over zeolites of different structure. J Catal 1994;147(2):494–9. https://doi.org/10.1006/jcat.1994.1166.
[70] Kistiakowsky GB, Nickle AG. Ethane-ethylene and propane-propylene equilibria. Discuss Faraday Soc 1951;10:175. https://doi.org/10.1039/DF9511000175.
[71] Kistiakowsky GB, Ruhoff JR, Smith HA, Vaughan WE. Heats of organic reactions. II. Hydrogenation of some simpler olefinic hydrocarbons. J Am Chem Soc 1935;57 (5):876–82. https://doi.org/10.1021/ja01308a025.
[72] Jan O, Resende FL. Liquid hydrocarbon production via ethylene oligomerization over Ni-Hβ. Fuel Process Technol 2018;179:269–76. https://doi.org/10.1016/j.fuproc.2018.07.004.
[73] Lee M, Yoon JW, Kim Y, Yoon JS, Chae H-J, Han Y-H, et al. Ni/SIRAL-30 as a heterogeneous catalyst for ethylene oligomerization. Appl Catal A 2018;562: 87–93. https://doi.org/10.1016/j.apcata.2018.06.004.
[74] Chen L, Li G, Wang Z, Li S, Zhang M, Li X. Ethylene oligomerization over nickel supported silica-alumina catalysts with high selectivity for C10+ products. Catalysts 2020;10(2):180. https://doi.org/10.3390/catal10020180.
[75] de Souza MO, de Souza RF, Rodrigues LR, Pastore HO, Gauvin RM, Gallo JMR, et al. Heterogenized nickel catalysts for propene dimerization: Support effects on activity and selectivity. Catal Commun 2013;32:32–5. https://doi.org/10.1016/j.catcom.2012.11.023.
[76] Wilshier KG, Smart P, Western R, Mole T, Behrsing T. Oligomerization of propene over H-ZSM-5 zeolite. Appl Catal 1987;31(2):339–59. https://doi.org/10.1016/S0166-9834(00)80701-0.
[77] A. N Mlinar, G. B Baur, G. G Bong, A. " Getsoian, A. T Bell. Propene oligomerization over Ni-exchanged Na-X zeolites. J Catal. 2012. 296:156–164. doi: 10.1016/j.jcat.2012.09.010.
[78] Cai T, Zang L, Qi A, Wang D, Cao D, Li L. Propene oligomerization catalyst derived from nickel sulfate supported on γ-alumina. Appl Catal 1991;69(1):1–13. https://doi.org/10.1016/S0166-9834(00)83287-X.
[79] Harms SM, Kojima M, O'Connor CT. Propene oligomerization over nickel-loaded silica-alumina. Fuel Process Technol 1989;21(3):231–43. https://doi.org/10.1016/0378-3820(89)90052-0.